Reflectivity and conductivity of $YBa_2Cu_3O_7$

R. T. Collins, Z. Schlesinger, F. Holtzberg, P. Chaudhari, and C. Feild
IBM Thomas J. Watson Research Center, Yorktown Heights, New York 10598
(Received 8 August 1988; revised manuscript received 6 January 1989)

We obtain the a-b plane infrared conductivity of $YBa_2Cu_3O_7$ from temperature-dependent reflectivity spectra of crystals and films with $T_c \simeq 92$ K. The normal state is characterized by a free-carrier band with an enhanced low-frequency mass and a frequency-dependent scattering rate, which indicate coupling to an excitation spectrum with a characteristic frequency scale of $\omega_c \lesssim 700$ cm^{-1} and coupling strength of $\lambda \simeq 2$ to 3.

The recent discovery of high-temperature superconductivity in layered copper oxide compounds[1,2] has been followed by a monumental effort to understand the physics of these systems. Crucial to that endeavor is the reliable measurement of fundamental properties in both the normal and superconducting states. Spectroscopic techniques, such as inelastic neutron scattering, tunneling, and infrared spectroscopy, are particularly important because they probe the spectrum of intermediate energy (i.e., 1 meV to 1 eV) excitations which may be crucial to the mechanism of high-temperature superconductivity. Probing these excitations with infrared requires precise measurements of the reflectivity and its temperature dependence, from which the dynamic conductivity $\sigma(\omega)$ is obtained.

A central question regarding the normal-state infrared properties[3-6] is whether the conductivity of the copper-oxygen planes is most appropriately described in terms of a dynamic interaction which leads to a frequency-dependent scattering rate and carrier mass, or as a superposition of a free-carrier band and some type of mid-infrared interband transition. These two approaches differ fundamentally since the former implies a strongly coupled normal state, while the latter is most consistent with a weak-coupling view. In this work we describe reflectivity measurements on the a-b plane of $YBa_2Cu_3O_7$ crystals and films with transitions at $T_c \simeq 92$ K. We find that either model can describe the reflectivity at a single temperature, but, in contrast with similar work on oxygen-deficient material,[6] we find significant temperature dependence in $R(\omega)$ and $\sigma(\omega)$ through the crucial mid-infrared region. This broad band temperature dependence is inconsistent with a mid-infrared band model, but is the expected behavior within a frequency-dependent scattering approach.

Our measurements were made on the a-b plane of oriented films of $YBa_2Cu_3O_7$ with relatively large areas ($\simeq 10$ mm^2) and on crystals of smaller area ($\simeq 2$ mm^2), with both as annealed and polished surfaces. The films were grown on $SrTiO_3$ substrates to a thickness of $\simeq 1$ μm. Both films and crystals were single phase. All of the samples were microtwinned so that an average of the a-b plane properties was obtained. ac susceptibility measurements showed the samples to have superconducting transitions at $\simeq 92$ K with widths less than 0.2 K for the crystals and of $\simeq 1$ K for the films. Reflectivity measurements were made at near normal incidence. Each sample was mounted in close proximity to an evaporated gold reference mirror which was carefully aligned parallel to the sample surface. A manipulator allowed either the sample or reference to be positioned in the infrared beam. We tested our technique by studying both brass-Au and Au-Au reflectivity ratios and in each case obtain accuracy of a few tenths of a percent.

We have measured the normal-state reflectivity of our samples for temperatures between 300 K and 95 K. In Fig. 1 we show spectra taken at 250 K (dots) and 100 K (triangles) for a polished face of one of our $YBa_2Cu_3O_7$ crystals. We see in Fig. 1 that the reflectivity increases over a very wide frequency range ($\simeq 100$–8000 cm^{-1}) as T is reduced in the normal state. Virtually identical spectra were observed for as annealed crystal faces. Although the films showed a slightly lower reflectivity ($\simeq 5\%$ lower at 4000 cm^{-1}) in the mid-infrared, they displayed the same temperature dependence as observed for the crystal samples. We note that when temperature was reduced below T_c the behavior changed dramatically. All of the samples discussed here showed a distinct gaplike increase in the low-frequency reflectivity which exhibits a clear onset at T_c with a characteristic energy scale of 7–8 kT_c as

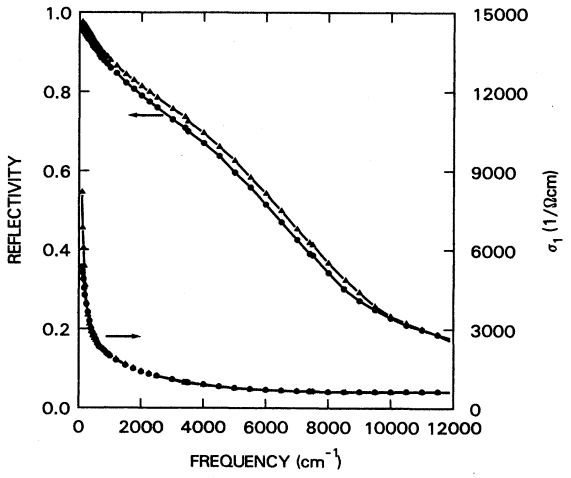

FIG. 1. The reflectivity and the real part of the conductivity of $YBa_2Cu_3O_7$ are shown for $T = 100$ K (triangles) and 250 K (dots) for ω up to 12000 cm^{-1}.

we have previously reported.[4]

Figure 1 also gives the real part of the conductivity, $\sigma_1(\omega)$, at 250 and 100 K, obtained by appending the high-frequency reflectivity data of Ref. 7 (12000–30000 cm^{-1}) onto our data (100–12000 cm^{-1}) and applying a Kramers-Kronig transform analysis to the resultant spectrum. Below 100 cm^{-1} the reflectivity was terminated with a Hagen-Rubens form and above 30000 cm^{-1} a $1/\omega^4$ termination was used. We obtain the plasma frequency from the f sum rule on $\sigma_1(\omega)$, which we integrate up to $\sim$20000 cm^{-1} after subtracting off a temperature-independent interband (Lorentz oscillator) contribution to $\sigma_1(\omega)$ centered at $\sim$2 eV. In this manner a plasma frequency of $\omega_p \simeq 22000$ cm^{-1} $\simeq$2.7 eV is obtained, corresponding to a ratio $n/m_b \simeq (5.5\times10^{21}\ cm^{-3})/m_e$ where n is the free-carrier concentration and m_b is the band mass, in agreement with previous results.[4]

In Fig. 2, the reflectivity (from Fig. 1) and the real (a) and imaginary (b) parts of $\sigma(\omega)$ are plotted for $\omega < 2500$ cm^{-1}. We can analyze the conductivity in terms of a frequency-dependent scattering model in which

$$\tilde{\sigma}(\omega) = \frac{ne^2\tau^*(\omega)}{m^*(\omega)[1-i\omega\tau^*(\omega)]}, \quad (1)$$

where $m^*(\omega) = m_b[1+\lambda(\omega)]$ is the renormalized mass and $\tau^*(\omega) = \tau(\omega)[1+\lambda(\omega)]$ is the renormalized scattering rate. Frequency-dependent scattering models have previously been used to treat electron-phonon interactions in ordinary metals[8,9] and spin-related excitations in heavy-fermion systems.[10,11]

In Fig. 3 we plot $\tau^{-1}(\omega)$ and $m^*/m_b - 1$, which are obtained using Eq. (1) with $n/m_b = (5.5\times10^{21}\ cm^{-3})/m_e$, and, like $\sigma_1(\omega)$ and $\sigma_2(\omega)$, are related by causality. The behavior shown in Figs. 3(a) and 3(b) can be understood as a consequence of an interaction of the charged carriers with an inelastic scattering spectrum. At low temperature and frequency the carriers have an enhanced mass because they drag an excitation cloud along with them, and the scattering rate is low since the inelastic scattering channels are not energetically available. With increasing frequency, the scattering rate increases as additional scattering channels become accessible, and the mass enhancement diminishes as the carriers shed their excitation cloud. In this manner an excitation spectrum which is not itself infrared active, but which is strongly coupled to the carriers, can dramatically influence the infrared (and dc) conductivity. In Fig. 3 the frequency dependence of $\tau^{-1}(\omega)$ is most rapid from about 200–700 cm^{-1}. Within the inelastic scattering approach, we associate this with the characteristic frequency of the excitation spectrum to which the carriers are coupled. The low-frequency value of $\lambda(\omega)$ at 100 K indicates an overall coupling strength of roughly $\lambda = 3$ to that spectrum. This

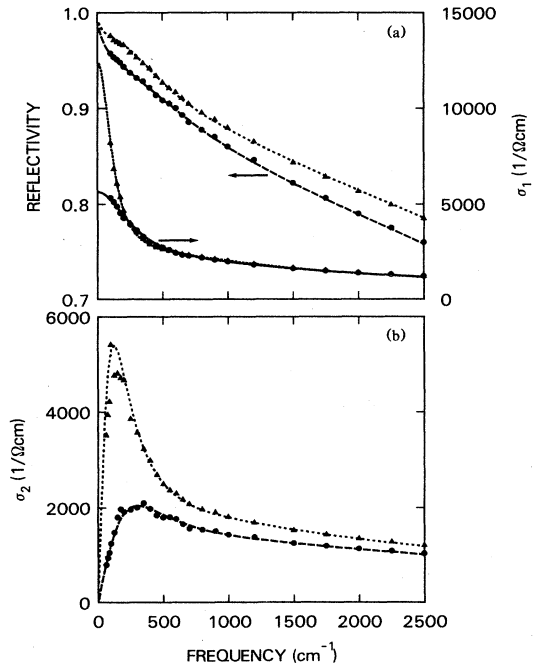

FIG. 2. The reflectivity and the real part of the conductivity of $YBa_2Cu_3O_7$ (a) and the imaginary part of the conductivity (b) are shown for $T = 100$ K (triangles) and 250 K (dots) for ω up to 2500 cm^{-1}. The lines through the data points refer to a frequency-dependent scattering model calculation described in the text.

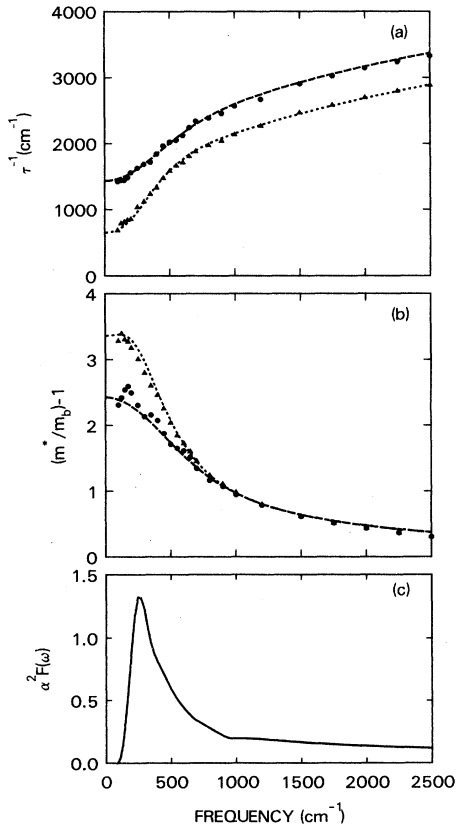

FIG. 3. (a) The unrenormalized scattering rate and (b) the reduced mass enhancement of $YBa_2Cu_3O_7$ are shown for $T = 100$ K (triangles) and 250 K (dots). The lines through the data points in (a) and (b) refer to a model calculation which uses the coupling spectrum $\alpha^2F(\omega)$ shown in (c).

coupling strength lies between that typical of the electron-phonon interaction ($\lambda \simeq 1$) and the very large values associated with "spin-fluctuation exchange" induced mass enhancements ($\lambda \simeq 50$) in moderately heavy electron systems such as UPt_3 and $CePd_3$.[10,11]

In our frequency-dependent scattering analysis of the conductivity in Fig. 2, we have assumed only a single free-carrier band. The low-frequency peak in $\sigma_1(\omega)$ in the 100-K conductivity is a direct consequence of the reduced scattering rate at frequencies less than the characteristic scattering energy. Bonn *et al.*[5] have suggested an alternative analysis of the *a-b* plane conductivity in which $\sigma_1(\omega)$ is divided into a low-frequency Drude peak with a frequency-independent scattering rate and a temperature-independent interband transition which is responsible for the mid-infrared conductivity. While we are able to fit this mid-infrared band model to our 100-K spectrum (with approximately $\frac{1}{5}$ of the area in the low-energy peak), we find that the temperature dependence predicted by the model is inconsistent with our observations. In particular, neither $R(\omega)$ nor $\sigma(\omega)$ is predicted to show temperature dependence for $\omega \gtrsim 1500$ cm^{-1} (in the part of the spectrum dominated by the interband transition). In a frequency-dependent scattering model there is a fundamental relationship between frequency and temperature dependence. To illustrate this, it is useful to introduce a coupling spectrum, $\alpha^2F(\omega)$, from which a scattering rate and mass enhancement are calculated as a function of frequency and temperature. In general, this is a nontrivial calculation that requires a detailed knowledge of the nature of the interaction. For the sake of simplicity, we approximate the optical scattering rate, $\tau^{-1}(\omega)$, by the quasiparticle lifetime averaged over the Fermi surface, and use (Ref. 12),

$$\tau^{-1}(\omega) = -2\,\mathrm{Im}\bar{\Sigma}(\omega) = \pi \int_0^\infty d\omega' \alpha^2F(\omega') f(\omega';T)\,, \quad (2)$$

where $\bar{\Sigma}(\omega)$ is the self-energy and

$$f(\omega';T) = \coth\left(\frac{\omega'}{2T}\right) - \tfrac{1}{2}\tanh\left(\frac{\omega'+\omega}{2T}\right) - \tfrac{1}{2}\tanh\left(\frac{\omega'-\omega}{2T}\right)$$

is an occupation factor related term which contains all of the temperature dependence in Eq. (2). Figure 3(c) shows a spectral function which provides a fit to both the temperature and frequency dependence of our data [dashed (250-K) and dotted (100-K) curves] in Figs. 2 and 3. [$m^*/m_b - 1$ is obtained from a Kramers-Kronig transform of $\tau^{-1}(\omega)$.] We have included an elastic contribution to $\tau^{-1}(\omega)$ of 560 cm^{-1}. The spectral function $\alpha^2F(\omega)$ obtained by this fitting procedure should be viewed only as a rough approximation to the true coupling spectrum. In particular, calculations which explicitly take into account the difference between the transport scattering rate and quasiparticle lifetime indicate that the spectral weight above 800 cm^{-1} should be ignored.[13] The integrated coupling strength in this high-frequency range is less than 1, and, hence, does not dramatically alter our estimate of the total coupling. These calculations also predict a somewhat larger temperature dependence than we observe. The salient point is that the temperature dependence exhibited by our data is qualitatively consistent with the presence of frequency-dependent scattering rather than with the mid-infrared mode-model. We cannot rule out the possibility that frequency-dependent scattering and a mid-infrared mode may both be present. This is a particularly interesting possibility in $YBa_2Cu_3O_7$ where the presence of localized carriers on the chains could give a modelike contribution to the mid-infrared. Reflectivity measurements in the near-infrared (>8000 cm^{-1}) already indicate that the *a* and *b* axis are inequivalent.[14] Separation of the *a-b* plane conductivity into chain and plane contributions will have to wait for studies of untwinned samples. At present we do not feel that the contributions of the chains will significantly alter the characteristic scattering frequency ($\lesssim 700$ cm^{-1}) although the mass enhancement may be reduced.

In models of transport in correlated systems potentially applicable to $YBa_2Cu_3O_7$, a mass enhancement such as we observe can arise from the interaction of the carriers with spin-related excitations associated with the Cu, for which the characteristic energy scale is set by the exchange interaction *J*. [In resonating valence bond (RVB) language this is the holon-spinon scattering.] For example, Kane, Lee, and Reed[15] have studied the motion of a hole in a large-*U* Hubbard model with either Néel or an RVB order, and obtain a mass enhancement of order t/J associated with coupling to spin excitations of characteristic energy *J*, where $4t$ is the hole bandwidth. In principle, strong electron-phonon coupling provides an alternative origin for our measured mass enhancement [the phonon density of states is roughly constant up to a cutoff frequency of about 600 cm^{-1} (Ref. 16)]. The observed coupling strength, $\lambda \sim 2$–3, however, would be unprecedented, particularly at such a high-frequency scale.

In Fig. 3 we have plotted $\tau^{-1}(\omega)$, however, the actual (renormalized) scattering rate is $\tau^{*-1}(\omega) = \tau^{-1}(\omega) m_b/m^*$. It is interesting to note that throughout our frequency range the inelastic contribution to $\hbar/\tau^{*-1}(\omega)$ is of order $kT + \hbar\omega$, suggesting a nearly localized Fermi liquid, or that $YBa_2Cu_3O_7$ is at the edge of the regime in which a Fermi liquid theory is well defined.

An examination of the correspondence between our infrared results and other measurable quantities is also useful. For example, using our measured values for ω_p and m^*/m_b we estimate the *a-b* plane London penetration depth to be $\lambda = (c/\omega_p)(m^*/m_b)^{1/2} \simeq 1400$ Å. Specific-heat measurements are also expected to exhibit the same mass enhancement as with the infrared. The correspondence between our infrared data and the dc conductivity can be examined using the measured low-frequency values of $\tau^{-1}(\omega)$ [Fig. 3(a)] in the $\omega = 0$ limit of Eq. (1), $\sigma_{dc} = ne^2\tau(0)/m_b$, from which we obtain 85, 105, 140, and 175 $\mu\Omega$ cm at $T = 100$, 150, 200, and 250 K, respectively. These values are comparable to typical measured dc resistivities on similar crystals. Although they appear to extrapolate roughly to the origin, there is actually some upward curvature which, in the model, leads to a positive intercept on the *y* axis.

Efforts to measure and interpret the *a-b* plane infrared

conductivity of crystalline $YBa_2Cu_3O_7$ began with Ref. 4, in which $\sigma_1(\omega)$ at room temperature and $\omega \gtrsim 1000$ cm^{-1} was reported, and shown to contain no strong 0.3–0.5 eV peak as reported in ceramic samples. Subsequent efforts extended this work to lower frequencies and temperatures,[5,6] where $\sigma_1(\omega)$ exhibits a temperature-dependent peak as shown in Fig. 2. Sulewski *et al.*[3] were the first to apply a frequency-dependent scattering model to the oxide superconductors in their study of ceramic $YBa_2Cu_3O_7$. More recently, Thomas *et al.*[6] have analyzed the *a-b* plane conductivity of O-deficient crystals ($T_c \simeq 50$–70 K) in terms of both the frequency-dependent scattering approach and mid-infrared band model. Their results differ fundamentally from ours in that they observe a much lower reflectance throughout the entire mid-infrared region and they find no temperature dependence above 1000 cm^{-1}, which, unlike our data, seems consistent with a mid-infrared-band model.[5] They emphasize the frequency-dependent scattering approach from which they obtain a coupling of $\lambda \simeq 9$, although, as they point out, their measured temperature dependence is not consistent with their carrier-oscillator model.[6]

In conclusion, we find that the frequency and temperature dependence of the normal-state transport of $YBa_2Cu_3O_7$ in the far-infrared region supports a frequency-dependent scattering rate arising from coupling to an excitation spectrum with a characteristic energy scale of $\simeq 200$–700 cm^{-1} and an integrated coupling strength of $\lambda \simeq 2$–3. This approach provides a unified description of both the temperature and frequency dependence of the transport behavior above T_c.

Note added in proof. Since the submission of this paper we have made measurements which suggest that part of the mid-infrared conductivity does arise from a source other than the free carriers in the planes (such as the chain related contributions mentioned above). Accounting for this does not appear to alter the characteristic scattering frequency ($\omega_c \simeq 200$–700 cm^{-1}) substantially, but does reduce our estimate for the unrenormalized plasma frequency (ω_p) which, in turn, can reduce our estimate of λ by as much as a factor of 2. We then obtain reasonable agreement between the measured temperature dependences and those calculated using the more sophisticated frequency dependent scattering approaches (13) mentioned above.

We would like to acknowledge excellent technical assistance from J. A. Calise, Gene Komsa, and John Sosik and valuable conversations with P. W. Anderson, H. Fukuyama, P. A. Lee, D. M. Newns, A. J. Sievers, and B. C. Webb. Insights developed over the last decade by A. J. Sievers and co-workers (including F. E. Pinkerton, B. C. Webb, and P. E. Sulewski) have been crucial to our present effort.

[1] J. G. Bednorz and K. A. Müller, Z. Phys. B **64**, 189 (1986).
[2] M. K. Wu, J. Ashburn, C. J. Torng, P. H. Hor, R. L. Meng, L. Gao, Z. J. Huang, Y. Q. Wang, and C. W. Chu, Phys. Rev. Lett. **58**, 908 (1987).
[3] P. E. Sulewski, T. W. Noh, J. T. McWhirter, A. J. Sievers, S. E. Russek, R. A. Buhrman, C. S. Jee, J. E. Crow, R. E. Salomon, and G. Myer, Phys. Rev. B **36**, 2357 (1987).
[4] Z. Schlesinger, R. T. Collins, D. L. Kaiser, and F. Holtzberg, Phys. Rev. Lett. **59**, 1958 (1987).
[5] D. A. Bonn, A. H. O'Reilly, J. E. Greedan, C. V. Stager, T. Timusk, K. Karamas, and D. B. Tanner, Phys. Rev. B **37**, 1574 (1988); T. Timusk, S. L. Herr, K. Kamarás, C. D. Porter, D. B. Tanner, D. A. Bonn, J. D. Garrett, C. V. Stager, J. E. Greedan, and M. Reedyk (unpublished).
[6] G. A. Thomas, J. Orenstein, D. H. Rapkine, M. Capizzi, A. J. Millis, R. N. Bhatt, L. F. Schneemeyer, and J. V. Waszczak (unpublished).
[7] K. Kamarás, C. D. Porter, M. G. Doss, S. L. Herr, D. B. Tanner, D. A. Bonn, J. E. Greedan, A. H. O'Reilly, C. V. Stager, and T. Timusk, Phys. Rev. Lett. **59**, 919 (1987).
[8] T. Holstein, Phys. Rev. **96**, 535 (1954).
[9] P. B. Allen, Phys. Rev. B **3**, 305 (1971).
[10] B. C. Webb, A. J. Sievers, and T. Mihalisin, Phys. Rev. Lett. **57**, 1951 (1986).
[11] P. E. Sulewski, A. J. Sievers, M. B. Maple, M. S. Torikachvili, J. L. Smith, and Z. Fisk, Phys. Rev. B **38**, 5338 (1988).
[12] A. J. Millis, Subir Sachdev, and C. M. Varma, Phys. Rev. B **37**, 4975 (1988).
[13] D. J. Scalapino, N. E. Bickers, Z. Schlesinger, and R. T. Collins (unpublished); A. J. Millis (unpublished).
[14] M. P. Petrov, A. I. Grachev, M. V. Krasin'kova, A. A. Nechitailov, V. V. Prokofiev, V. V. Poborchy, S. I. Shagin, and N. F. Kartenko, Solid State Commun. **67**, 1197 (1988).
[15] C. L. Kane, P. A. Lee, and N. Read (unpublished).
[16] B. Renker, E. Gering, G. Roth, W. Reichardt, D. Ewert and H. Rietschel (unpublished).